

COMMENTARY

 OPEN ACCESS

## Selective binding and lateral clustering of $\alpha 5 \beta 1$ and $\alpha v \beta 3$ integrins: Unraveling the spatial requirements for cell spreading and focal adhesion assembly

Viktoria Schaufler<sup>a,b</sup>, Helmi Czichos-Medda<sup>a,b</sup>, Vera Hirschfeld-Warnecken<sup>a,b</sup>, Stefanie Neubauer<sup>c</sup>, Florian Rechenmacher<sup>c</sup>, Rebecca Medda<sup>a,b</sup>, Horst Kessler<sup>c</sup>, Benjamin Geiger<sup>d</sup>, Joachim P. Spatz<sup>a,b</sup>, and E. Ada Cavalcanti-Adam<sup>a,b</sup>

<sup>a</sup>Department of New Materials and Biosystems, Max Planck Institute for Intelligent Systems, Stuttgart, Germany; <sup>b</sup>Department of Biophysical Chemistry, Institute of Physical Chemistry, University of Heidelberg, Heidelberg, Germany; <sup>c</sup>Institute for Advanced Study and Center for Integrated Protein Science, Department of Chemistry, Technical University Munich, Garching, Germany; <sup>d</sup>Department of Molecular Cell Biology, Weizmann Institute of Science, Rehovot, Israel

### ABSTRACT

Coordination of the specific functions of  $\alpha 5 \beta 1$  and  $\alpha v \beta 3$  integrins is crucial for the precise regulation of cell adhesion, spreading and migration, yet the contribution of differential integrin-specific crosstalk to these processes remains unclear. To determine the specific functions of  $\alpha v \beta 3$  and  $\alpha 5 \beta 1$  integrins, we used nanoarrays of gold particles presenting immobilized, integrin-selective peptidomimetic ligands. Integrin binding to the peptidomimetics is highly selective, and cells can spread on both ligands. However, spreading is faster and the projected cell area is greater on  $\alpha 5 \beta 1$  ligand; both depend on ligand spacing. Quantitative analysis of adhesion plaques shows that focal adhesion size is increased in cells adhering to  $\alpha v \beta 3$  ligand at 30 and 60 nm spacings. Analysis of  $\alpha v \beta 3$  and  $\alpha 5 \beta 1$  integrin clusters indicates that fibrillar adhesions are more prominent in cells adhering to  $\alpha 5 \beta 1$  ligand, while clusters are mostly localized at the cell margins in cells adhering to  $\alpha v \beta 3$  ligand.  $\alpha v \beta 3$  integrin clusters are more pronounced on  $\alpha v \beta 3$  ligand, though they can also be detected in cells adhering to  $\alpha 5 \beta 1$  ligand. Furthermore,  $\alpha 5 \beta 1$  integrin clusters are present in cells adhering to  $\alpha 5 \beta 1$  ligand, and often colocalize with  $\alpha v \beta 3$  clusters. Taken together, these findings indicate that the activation of  $\alpha v \beta 3$  integrin by ligand binding is dispensable for initial adhesion and spreading, but essential to formation of stable focal adhesions.

### ARTICLE HISTORY

Received 19 January 2016  
Revised 1 March 2016  
Accepted 4 March 2016

### KEYWORDS

block copolymer micellar nanolithography; focal adhesion; integrin crosstalk; integrins; peptidomimetic; receptor clustering; surface nanopatterning

## Introduction

Cell-extracellular matrix (ECM) interactions, mediated by integrins, are crucial for cell adhesion, migration, proliferation and differentiation. Upon binding to ECM proteins, the lateral clustering of integrins and the recruitment of intracellular adhesion proteins to the attachment site leads to the formation of focal adhesions (FAs) and the assembly of actin stress fibers.<sup>1</sup> Various integrin types participate in the formation and maturation of FAs. Notably, FA formation involves several integrins (e.g.,  $\alpha 5 \beta 1$  and  $\alpha v \beta 3$ ), each of which is known to perform a different function.<sup>2–4</sup>


The selective enrichment of  $\alpha 5 \beta 1$  integrins in fibrillar adhesions, which arise from mature FAs following the centripetal translocation of the receptors, is important for fibronectin fibrillogenesis, whereas  $\alpha v \beta 3$  integrins remain in FAs, exerting stabilizing functions.<sup>2,3,5–7</sup>

Accordingly, it was proposed that this localization pattern and segregation could be due to the specific mechanotransduction functions and signaling pathways associated with  $\alpha 5 \beta 1$  and  $\alpha v \beta 3$  integrins. Thus, identification of the integrin-specific triggers for specific biochemical and biomechanical changes in FAs remain a challenge, necessitating novel methods that differentially control integrin activation and localization.

The functional diversity of  $\alpha 5 \beta 1$  and  $\alpha v \beta 3$  integrins has been shown through their regulation of cell adhesion forces. The catch bond established by  $\beta 1$  integrin with fibronectin might adjust adhesion strength according to the underlying mechanical tension, while  $\alpha v \beta 3$  integrin binding enables the structural reinforcement of the integrin-actin linkage.<sup>4,8</sup> Downstream signaling requires the

**CONTACT** Joachim P. Spatz  [spatz@is.mpg.de](mailto:spatz@is.mpg.de); E. Ada Cavalcanti-Adam  [Ada.cavalcanti-adam@is.mpg.de](mailto:Ada.cavalcanti-adam@is.mpg.de)  Max Planck Institute for Intelligent Systems, Department of New Materials and Biosystems, Heisenbergstr. 3, D-70569 Stuttgart, Germany  Institute of Physical Chemistry, Department of Biophysical Chemistry, Im Neuenheim Feld 253, D-69120 Heidelberg, Germany.

Color versions of one or more of the figures in the article can be found online at [www.tandfonline.com/kcam](http://www.tandfonline.com/kcam).

 Supplemental material data for this article can be accessed on the publisher's website.

© 2016 Viktoria Schaufler, Helmi Czichos-Medda, Vera Hirschfeld-Warnecken, Stefanie Neubauer, Florian Rechenmacher, Rebecca Medda, Horst Kessler, Benjamin Geiger, Joachim P. Spatz, and E. Ada Cavalcanti-Adam. Published with license by Taylor & Francis.

This is an Open Access article distributed under the terms of the Creative Commons Attribution-Non-Commercial License (<http://creativecommons.org/licenses/by-nc/3.0/>), which permits unrestricted non-commercial use, distribution, and reproduction in any medium, provided the original work is properly cited. The moral rights of the named author(s) have been asserted.

cooperation of both integrin types, since expression of both  $\alpha v$ - and  $\alpha 5\beta 1$  integrins is necessary to induce myosin II activation in rigidity sensing and migration signaling.<sup>9-11</sup> An increase in cell traction forces is due to local activation of  $\beta 1$  but not  $\beta 3$  integrins; however, enhancing the expression of  $\alpha v\beta 3$  integrin can compensate for the loss of  $\alpha 5\beta 1$  integrin in force transmission.<sup>12-14</sup>

Specific activation of  $\alpha 5\beta 1$  and  $\alpha v\beta 3$  integrins in adhesion-mediated responses has thus far been investigated either by culturing cells on specific ECM proteins, by altering their expression profile, or by using RGD-based antagonists.<sup>3,5,9,15</sup> Recently, material surfaces for *in vitro* studies have been coated with highly selective compounds that bind and specifically activate  $\alpha 5\beta 1$  or  $\alpha v\beta 3$  integrins.<sup>13,16-18</sup> Ligand immobilization and receptor activation are prerequisites for  $\alpha v\beta 3$  integrin clustering and  $\beta 1$  integrin activation within FAs.<sup>19,20</sup>

To control the clustering of integrins we have developed surface patterning strategies that enable the presentation of integrin ligands at high spatial resolution.<sup>21,22</sup> (Given that spacing below 60 nm promotes and stabilizes FA formation, we recently determined that RGD ligand spacing modulates  $\beta 3$  integrin activation and force transmission.<sup>23</sup> Here, we combine tunable ligand spacing by surface patterning with the immobilization of  $\alpha 5\beta 1$  or  $\alpha v\beta 3$  integrin selective ligands,<sup>16</sup> to show that  $\alpha 5\beta 1$  integrin clustering enhances cell spreading, and is dependent on ligand spacing: only at spacings below 60 nm, mature FAs are formed. Furthermore,  $\alpha v\beta 3$  integrin clustering is essential to this process.

## Results

### **Cell adhesion to $\alpha 5\beta 1$ integrin selective ligands leads to faster spreading, and an increase in projected cell area**

We first monitored human osteosarcoma U2OS cells spreading on nanopatterned surfaces with gold nanoparticles spaced 30, 60, or 90 nm apart, and functionalized with either  $\alpha 5\beta 1$  or  $\alpha v\beta 3$  integrin selective ligands. Cell spreading kinetics during the first 60 min of adhesion is shown in Fig. 1 (see also Supplementary Movies 1-6, and Fig. S1). The smaller spacing led to a marked increase in cell spreading velocity and projected cell area, compared to cell spreading on substrates with larger spacings, regardless of the type of ligand immobilized on the surfaces. At distances of 30 nm and 60 nm, the projected cell area was greater, and its progression faster, when cells bound to the surface via  $\alpha 5\beta 1$  integrins (Fig. 1A and B and Fig. S1). Such differences were not observed on the substrate with 90 nm particle spacing (Fig. 1A). Moreover, the maximal area of cells adhering to  $\alpha 5\beta 1$  integrin ligands at 30 nm spacing was significantly greater than

that displayed by cells adhering to  $\alpha v\beta 3$  integrin ligands at that spacing (Fig. 1B). As the interparticle spacing increased, the maximal cell area of cells adhering to either ligand became comparable.

### **Cells adhering to the selective $\alpha v\beta 3$ integrin ligands form larger focal adhesions**

To determine the effects of integrin type and integrin lateral spacing on focal adhesion size and composition, cells were immunostained for vinculin, phospho-paxillin (PY118), and actin after 4 hr of adhesion to the surfaces (Fig. 2). Notably, cells formed peripheral FAs when adhering to  $\alpha v\beta 3$  integrin ligands, and fibrillar structures when adhering to the  $\alpha 5\beta 1$  integrin ligand. Vinculin clusters were larger in cells adhering to the  $\alpha v\beta 3$  integrin ligand at all spacings, compared to clusters formed on the  $\alpha 5\beta 1$  integrin ligand (Fig. 2A, and Fig. 2B, box plot). Significant differences in vinculin cluster size are observed only in cells adhering to the  $\alpha v\beta 3$  integrin ligand at 30 and 60 nm spacings (Fig. 2A, small inserts left and middle), whereas at the 90 nm spacing, only a small increase in cluster size was seen, compared to cells adhering to the  $\alpha 5\beta 1$  integrin ligand (Fig. 2A small inserts right).

The phosphorylation of paxillin promotes the assembly of focal adhesions, while non-phosphorylated paxillin is commonly associated with fibrillar adhesions.<sup>24</sup> In FAs, paxillin phosphorylation of cells adhering to the 2 different integrin ligands shows a similar trend (Fig. 2A and Fig. 2C, box plot). For each integrin ligand type, however, the spacing between gold nanoparticles affects paxillin phosphorylation. In cells adhering to the  $\alpha v\beta 3$  integrin ligand, a significant difference in paxillin tyrosine phosphorylation is observed between cells adhering to substrates with all 3 interparticle spacings, while for the  $\alpha 5\beta 1$  integrin ligand, such a difference is observed only when comparing the 60 nm and 90 nm spacings.

It is noteworthy that activities promoting differential spreading and focal adhesion organization, both induced by  $\alpha v\beta 3$  and  $\alpha 5\beta 1$  integrin ligands on nanopatterns, can readily be obtained with the generic adhesive proteins vitronectin and fibronectin, respectively. This is illustrated in Fig. S2, showing spreading and FA formation patterns similar to those described above, based on labeling of the cells for diverse plaque proteins. In this experiment, cells adhering to fibronectin and vitronectin coatings were further treated with inhibitory antibodies that block  $\alpha v\beta 3$  and  $\alpha 5\beta 1$  adhesion, respectively. It was further shown that when both integrins were allowed to interact with the matrix, the “ $\alpha 5\beta 1$  phenotype” was dominant.

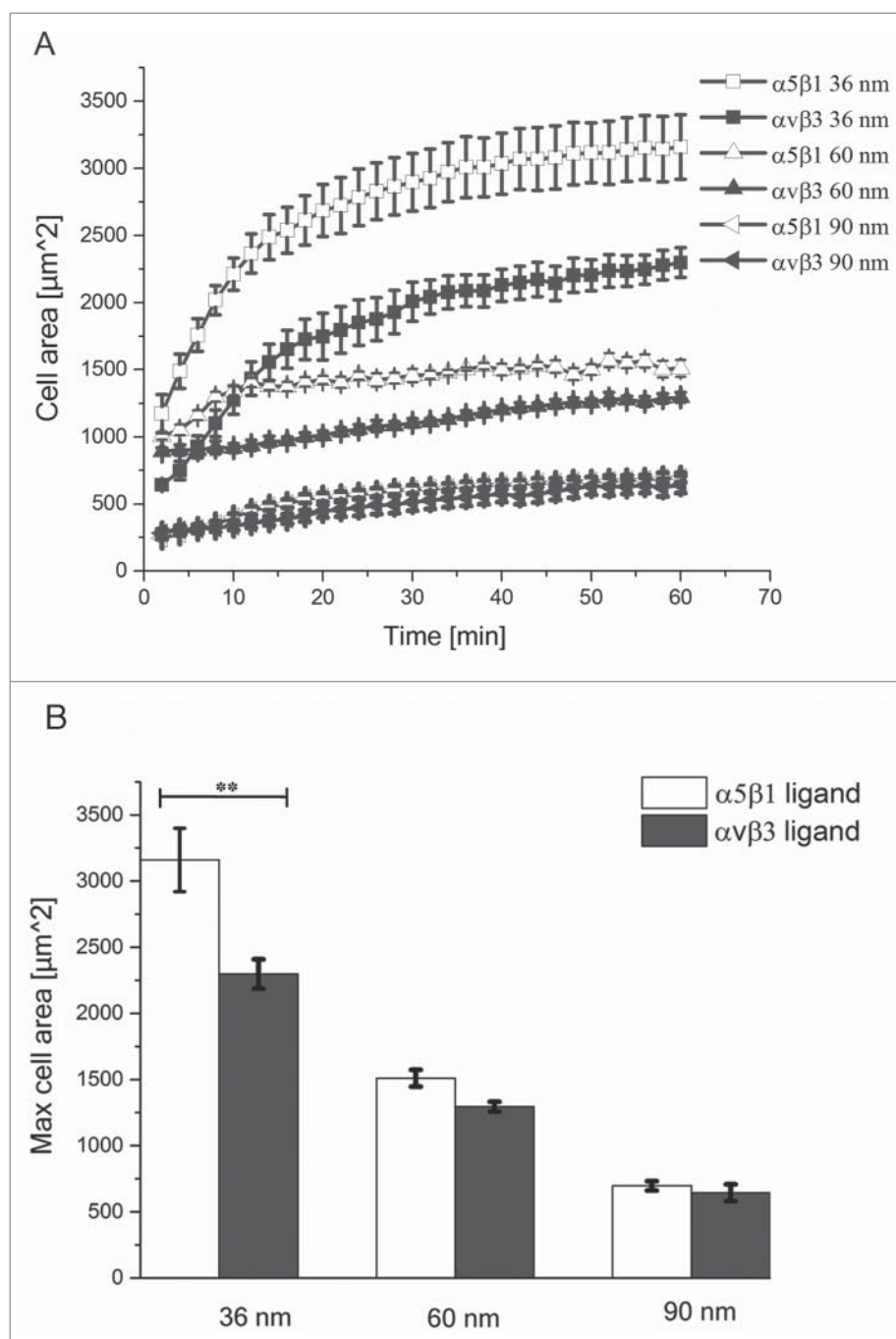


**Figure 1.** Cell spreading kinetics on nanopatterned surfaces functionalized with integrin selective ligands. (A) Progression of projected cell area during spreading on nanopatterned surfaces with interparticle distances of 30, 60, or 90 nm, and functionalized with  $\alpha 5\beta 1$  (white) and  $\alpha v\beta 3$  (black) integrin selective ligands. (B) Maximum projected cell area on the different surfaces. Error bars indicate SEM of 3 independent repeats.

#### ***$\alpha v\beta 3$ integrin clusters are present in cells adhering to the $\alpha 5\beta 1$ integrin selective ligand***

We next utilized indirect immunofluorescence staining and expression of fluorescence proteins to study the localization patterns of  $\alpha 5$  and  $\alpha v\beta 3$  integrins in cells adhering to nanopatterned surfaces presenting  $\alpha 5\beta 1$  and  $\alpha v\beta 3$  integrin selective ligands (Fig. 3, and

Supplementary Movies 7 and 8). Representative cells adhering to  $\alpha 5\beta 1$  or  $\alpha v\beta 3$  integrin ligands are shown in Fig. 3A for the 30 nm spacing, and in Fig. 3B for the 60 nm spacing. Cells adhering to the 90 nm nanopatterns are not shown, since the integrin clusters were hardly detectable, and the small focal adhesion clusters that did form were essentially identical for both ligands (Fig. 2).

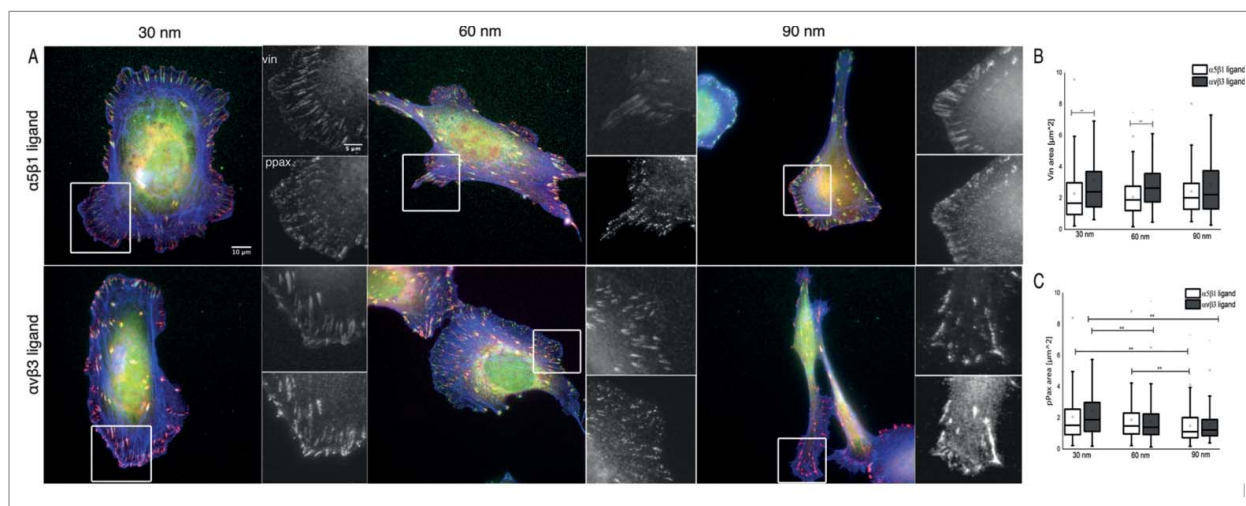


**Figure 2.** Focal adhesions in cells adhering to nanopatterned surfaces functionalized with integrin  $\alpha 5 \beta 1$  and  $\alpha v \beta 3$  integrin selective ligands. (A) Indirect immunofluorescence staining of vinculin (green), phosphorylated paxillin (red), and actin (blue) in U2OS cells. Insets are a magnification of separate stainings for vinculin and phosphorylated paxillin, in the cell region delineated by the white box. Cells adhering for 4 hr to  $\alpha 5 \beta 1$  (first row) and  $\alpha v \beta 3$  integrin selective ligands (second row) at spacings of 30 nm (left), 60 nm (middle), and 90 nm (right) were imaged by wide-field microscopy. (B) Analysis of vinculin cluster size; and (C) Analysis of phosphorylated paxillin (PY118) cluster size in U2OS cells. Box plots indicate cluster area values between 25% and 75%, and whiskers between 10% and 90% of the data range. The line in the box plot indicates the median value.  $p^* < 0.001$ .

Interestingly,  $\alpha v \beta 3$  integrin clusters were observed in all cells adhering to the 2 integrin selective ligands, regardless of particle spacing (Fig. 3A and B, lower middle panel), similar to cells adhering to fibronectin-coated surfaces (Fig. S3A, upper row). At the 30 nm spacing,  $\alpha v \beta 3$  and  $\alpha 5$  integrin clusters assembled and colocalized at the periphery of cells adhering to the  $\alpha 5 \beta 1$  integrin selective ligand. When adhering to a 60 nm-spaced nanopatterned surface,  $\alpha v \beta 3$  integrin clusters were still present, though smaller in size, compared to those on the 30 nm-spaced surface. In cells adhering to the  $\alpha v \beta 3$  integrin selective ligand, only  $\alpha v \beta 3$  integrin clusters were present, since  $\alpha 5$  staining appears very diffuse, and very few fibrillar adhesions were observed (Fig. 3A and B, lower left panel). The assembly of  $\alpha v \beta 3$  integrin clusters was comparable to that observed in cells adhering to vitronectin-coated surfaces (Fig. S3A, lower row).

#### **Inhibition of $\alpha v \beta 3$ integrins does not impair adhesion and spreading, but hinders focal adhesion assembly**

Integrins that are not bound to the immobilized ligands can still be recruited to focal adhesions via their cytoplasmic components, as was previously shown, using chimeric integrins, in which different integrin transmembrane and cytoplasmic domains were fused to an irrelevant extracellular domain.<sup>25</sup> Given that integrin can be recruited to FAs *via* their cytoplasmic domains, we further investigated the specific contribution of  $\alpha v \beta 3$

integrin recruitment for adhesion and FA assembly, by means of integrin function blocking. Here, prior to being seeded on the surfaces, cells in suspension were incubated with the soluble form of the peptidomimetic ligands, which selectively bind to  $\alpha 5 \beta 1$  or  $\alpha v \beta 3$  integrins, but lack the thiol group that binds to the gold nanopatterns.<sup>26</sup> Thus, the receptors are still physically present on the cell membrane, yet the selective ligand binds to them, and inhibits their function.

Blocking of  $\alpha 5 \beta 1$  integrins in U2OS cells plated on the  $\alpha 5 \beta 1$  integrin selective ligand inhibited adhesion, whereas blocking of  $\alpha v \beta 3$  integrins did not affect the adhesion of U2OS cells on these substrates (Fig. 4A, upper row). Accordingly, cells adhering to the  $\alpha v \beta 3$  integrin selective ligand could still attach and spread when  $\alpha 5 \beta 1$  integrins were blocked, whereas no cell adhesion was observed when  $\alpha v \beta 3$  integrins were blocked (Fig. 4A, lower row). Thus, the ligands mediated by either integrin type proved to be specific for adhesion.

We next performed staining for  $\alpha 5 \beta 1$  and  $\alpha v \beta 3$  integrins in U2OS cells, in which  $\alpha 5 \beta 1$  and  $\alpha v \beta 3$  integrins were pre-blocked with selective ligands (Fig. 4B). Interestingly,  $\alpha v \beta 3$  integrin blocking did not impair cell adhesion and spreading, but both  $\alpha 5 \beta 1$  and  $\alpha v \beta 3$  integrin clusters were not observed in U2OS cells adhering to the  $\alpha 5 \beta 1$  integrin selective ligand (Fig. 4B, upper row). Blocking of  $\alpha 5 \beta 1$  integrins in cells adhering to  $\alpha v \beta 3$  integrin selective ligands does not impair neither adhesion and spreading, nor assembly of  $\alpha v \beta 3$  integrin clusters (Fig. 4B, lower row). Similarly, in cells adhering to

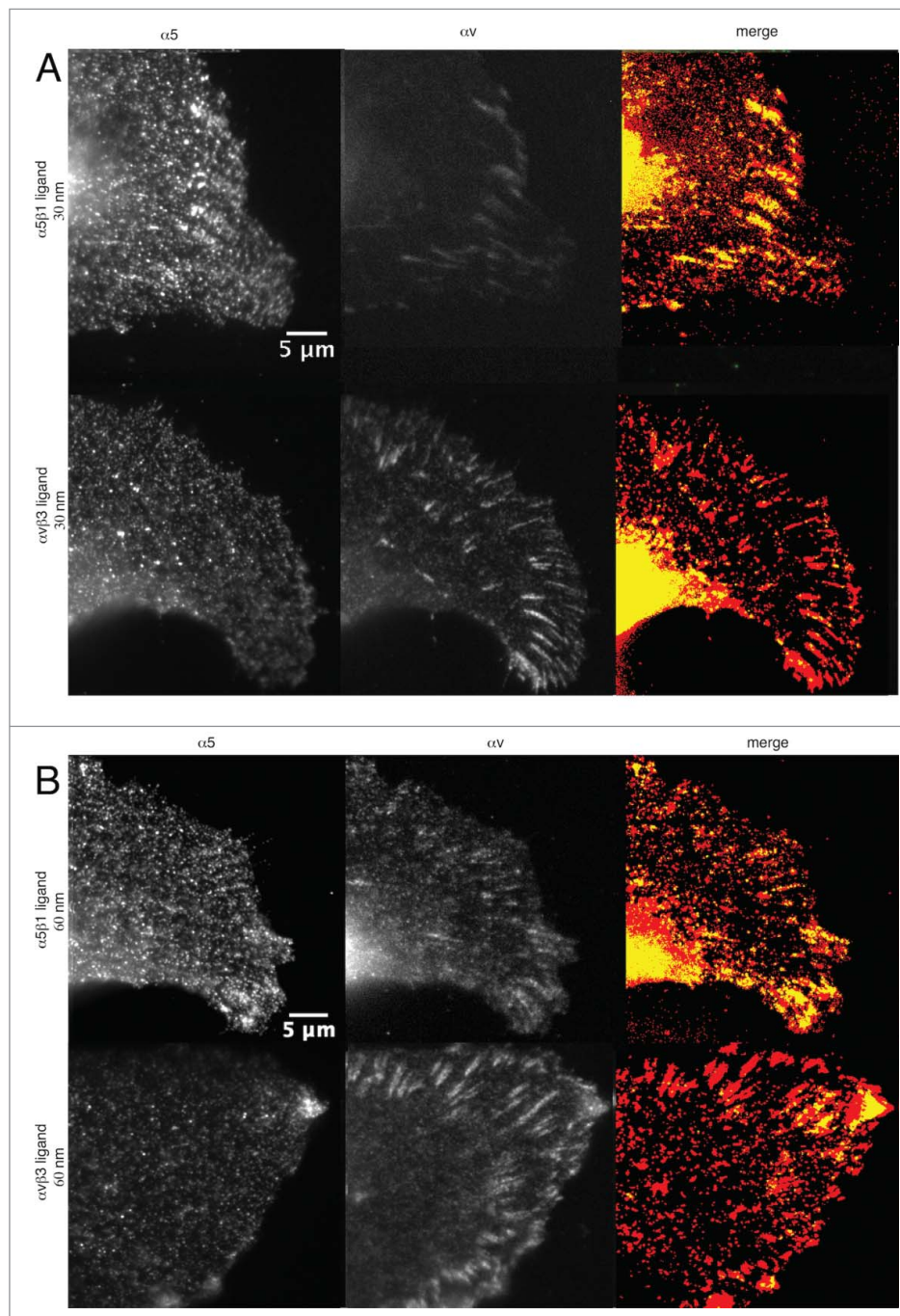


**Figure 3.**  $\alpha 5$  and  $\alpha v\beta 3$  clusters in U2OS cells adhering to nanopatterned surfaces functionalized with  $\alpha 5\beta 1$  and  $\alpha v\beta 3$  integrin selective ligands. (A) Cells adhering to surfaces with 30 nm interparticle spacing; and (B) Cells adhering to surfaces with 60 nm particle spacing. Upper row: Cells adhering to  $\alpha 5\beta 1$  integrin selective ligands. Lower row: Cells adhering to  $\alpha v\beta 3$  integrin selective ligands. Left: Staining for  $\alpha 5$  clusters. Middle: Staining for  $\alpha v\beta 3$  clusters. Right: Lookup table displaying the colocalization of  $\alpha 5$  and  $\alpha v\beta 3$  integrin clusters (pixel with positive signals for both integrins are shown in yellow).

vitronectin we blocked  $\alpha 5\beta 1$  integrin to prevent integrin binding to secreted fibronectin (Fig. S3B, middle row). Thus, in this condition cell adhesion is mediated only by  $\alpha v\beta 3$  integrin, while  $\alpha 5\beta 1$  integrin clustering is inhibited. We observed that adhesion and spreading were less efficient than in cells plated on fibronectin (Fig. S3B, upper row) since cells appear smaller and less cells could

attach to the substrate, but  $\alpha v\beta 3$  integrin clusters were present at the cell periphery. When plated on a mixture of fibronectin and vitronectin, spreading and formation of both  $\alpha 5\beta 1$  and  $\alpha v\beta 3$  integrin clusters was restored (Fig. S3B, lower row).

These results suggest that the adhesion of cells to specific ECM proteins influences cell spreading and integrin

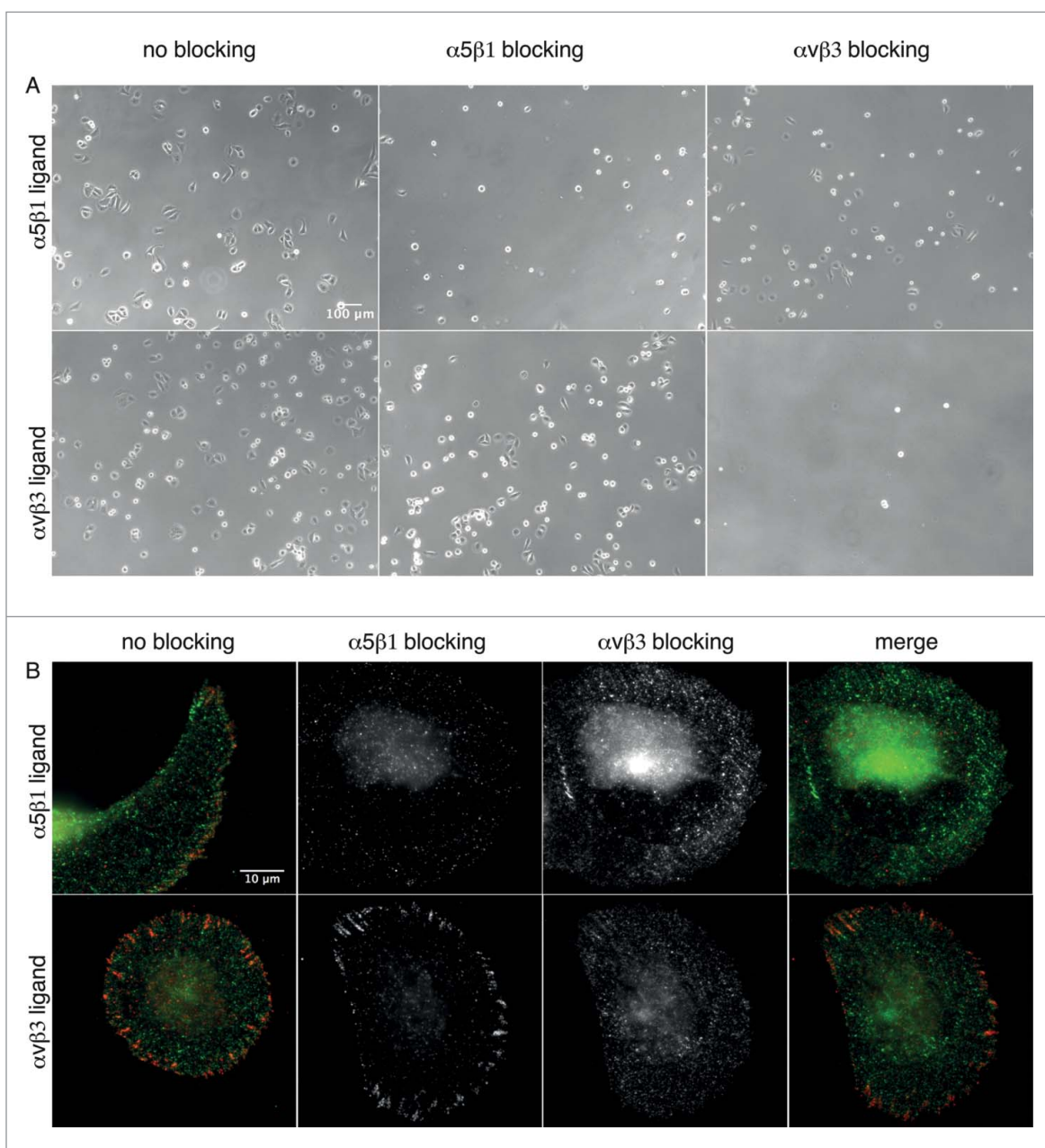


**Figure 4.**  $\alpha 5 \beta 1$  and  $\alpha v \beta 3$  integrin blocking. (A) Phase contrast micrographs of U2OS cells incubated with  $\alpha 5 \beta 1$  and  $\alpha v \beta 3$  integrin selective ligands, and seeded on nanopatterned surfaces functionalized with these ligands. Upper row: Cells adhering to  $\alpha 5 \beta 1$  integrin selective ligands. Lower row: Cells adhering to  $\alpha v \beta 3$  integrin selective ligands. Left: No integrin blocking. Middle:  $\alpha 5 \beta 1$  integrin blocking. Right:  $\alpha v \beta 3$  integrin blocking. (B) Indirect immunofluorescence staining of  $\alpha 5$  (green) and  $\alpha v \beta 3$  clusters (red) in U2OS cells pre-incubated with the integrin selective ligands. Cells were seen to adhere to nanopatterned surfaces functionalized with  $\alpha 5 \beta 1$  (upper row) and  $\alpha v \beta 3$  integrin selective ligands (lower row).

clustering, where  $\alpha 5 \beta 1$  integrin is important for the initial spreading and  $\alpha v \beta 3$  integrin supports the stabilization of FAs.

## Discussion

In this study, we aimed to elucidate the differential effects of matrix adhesion via  $\alpha 5 \beta 1$  and  $\alpha v \beta 3$  integrins on cell spreading and FA assembly. To that end, we

applied surface nanopatterning consisting of 8 nm-sized gold nanoparticles with interparticle spacings of 30, 60 or 90 nm, and functionalized with  $\alpha 5 \beta 1$  and  $\alpha v \beta 3$  integrin selective ligands.<sup>16,21</sup> On such surfaces, it is possible to control the binding sites of single integrins to the surface, and to modulate the lateral clustering of the receptors during cell adhesion.

Previously, we demonstrated that a  $\leq 60$  nm separation of gold nanoparticles functionalized with cyclic RGD

ligands favors cell adhesion and focal adhesion assembly, as a sufficient number of ligands are available for interactions with the receptors.<sup>21,27</sup> Furthermore, we determined that at a spacing of  $\geq 70$  nm, cells exhibited increased motility and focal adhesion instability, resulting in excessive retraction events.<sup>22</sup> More recently, by combining surface nanopatterning with molecular tension probes, we could show that the lateral clustering of integrins affects integrin tension at single bonds with RGD ligands, a process tightly coupled to actomyosin-driven tension.<sup>23</sup> However, this critical nanoscale spacing between cyclic RGD peptides left unclear the question whether the  $\alpha 5\beta 1$  and/or  $\alpha v\beta 3$  integrins that recognize these ligands, would cooperate and contribute in a manner similar to the formation of focal adhesions upon modulation of integrin clustering. Toward this aim,  $\alpha 5\beta 1$  and  $\alpha v\beta 3$  integrin selective peptidomimetics have been developed and linked to gold and titanium substrates to test the specific adhesion of  $\alpha 5\beta 1$  or  $\alpha v\beta 3$ -expressing fibroblasts to the prepared surfaces.<sup>18,28</sup> The use of such selective ligands for cell adhesion studies is a powerful means to determine the different functions of these integrin types, without perturbing the expression of the cell receptors themselves.<sup>3</sup>

The effects on cell adhesion dynamics and focal adhesion formation, seen following selective  $\alpha 5\beta 1$  or  $\alpha v\beta 3$  integrin clustering, reveal major differences between the 2 integrins. Although delayed and reduced spreading on surfaces with 90 nm particle spacings is still observed for both ligands, spreading kinetics are enhanced in cells adhering to the  $\alpha 5\beta 1$  integrin selective ligand at spacings of 30 and 60 nm, whereas spreading of cells adhering to the  $\alpha v\beta 3$  integrin selective ligand remains slower (Fig. 1 and Fig. S1). As shown in the kymograph analysis, the increased spreading in cells that bind to the  $\alpha 5\beta 1$  integrin selective ligand is due to increased lamellipodial protrusions. Thus, at the cellular level, adhesion dynamics to the selective ligands reflect that previously observed for cell adhesion to fibronectin and vitronectin coatings.<sup>6</sup>

The possibility that increased spreading mediated by  $\alpha 5\beta 1$  integrin binding dominates over  $\alpha v\beta 3$  integrins, rather than blocking of spreading being dominant, is validated by observations that spreading of cells plated on mixed fibronectin and vitronectin coatings resembles that occurring on fibronectin (Baruch Zimmerman, unpublished findings; and Fig. S3). Charo IF et al.<sup>29</sup> suggested that the increased spreading on fibronectin is due to the cooperative effect of  $\alpha 5\beta 1$  and  $\alpha v\beta 3$  integrins in promoting recognition and binding to fibronectin. The kinetics of spreading and formation of protrusions at the cell edges regulate cell traction forces,<sup>30</sup> which are dependent on  $\beta 1$  integrin activation, as determined by means of knockout cells, blocking approaches, and selective binding of this integrin type to specific ligands.<sup>12,13</sup> The

reinforcing behavior of  $\beta 1$  integrin bonds appears to be necessary for spreading, since reduced surface expression of  $\alpha 5\beta 1$  integrins negatively impacts spreading and stress fiber formation, but increases cortical actin assembly.<sup>31</sup>

Here, we observed that blocking  $\alpha 5\beta 1$  integrins in cells adhering to the  $\alpha v\beta 3$  integrin selective ligand, and blocking  $\alpha v\beta 3$  integrins in cells adhering to the  $\alpha 5\beta 1$  integrin selective ligand, do not impair cell adhesion and spreading. Rather, both  $\alpha 5\beta 1$  and  $\alpha v\beta 3$  integrin clusters are negatively affected only when  $\alpha v\beta 3$  integrin is blocked; i.e., that  $\alpha 5\beta 1$  selective adhesion to  $\alpha 5\beta 1$  ligands is not sufficient for focal adhesion formation when  $\alpha v\beta 3$  is blocked, and cannot be part of the adhesion cluster (Fig. 4, as compared with Fig. 3A). Also,  $\alpha v\beta 3$  alone cannot form clusters on the  $\alpha 5\beta 1$  ligand, when  $\alpha 5\beta 1$  is blocked (Fig. 4B).

A feedback mechanism involving integrin clustering and traction force generation may underlie mechanotransduction. Recently, Balcioglu HE et al.<sup>14</sup> reported that  $\alpha v\beta 3$  integrin-mediated adhesion enables FA assembly even at low matrix stiffness, while traction force magnitude remains unvaried. It could be speculated that activated  $\alpha v\beta 3$  integrins might be important in traction force modulation, which is intimately tied to receptor lateral spacing and FA assembly. In fact,  $\alpha v\beta 3$  integrin cluster size appears to be dependent on such spacing, since clusters forming on surfaces with 30 nm particle spacing, are larger than those seen with 60 nm-spaced particles (Fig. 3). Moreover, our observations that vinculin cluster size is modulated by particle spacing on both integrin ligands, and that the clusters are larger in cells adhering to the  $\alpha v\beta 3$  integrin selective ligand, indicate that FAs are more stable and turnover might be reduced. The larger vinculin clusters in cells adhering to  $\alpha v\beta 3$  integrin implies also that higher forces might be present in these cells and contribute also to the stability of FAs, since vinculin is in the force-transducing layer and regulates force transmission within FAs (Fig. 2).<sup>23,32</sup> On the contrary, FA signaling appears to be independent of the type of integrin bound to the surface, as indicated by staining for phosphorylated paxillin clusters (Fig. 2).

The fine-tuning of FA assembly might due to the following factors: (i) lateral spacing between single integrins and their clustering; (ii) the type of integrin recruited; and (iii) spatial distribution of different integrin types in FAs. The driving force behind  $\alpha v\beta 3$  integrin lateral association requires a certain density of activated proteins to maintain both the cluster, and FA stability.<sup>19</sup> Rossier O. et al.<sup>7</sup> reported that within FAs,  $\beta 1$  and  $\beta 3$  exhibit distinct dynamics at the nanoscale, due to differences in the relative amounts of each integrin type: the  $\beta 3$  immobile fractions are most abundant in FAs due to bond formation with talin and F-actin, whereas  $\beta 1$  integrins are less

enriched, and exhibit rearward movements. The coupling of  $\alpha v\beta 3$  integrins with F-actin, and the observation of ventral F-actin waves, suggest a dependence on the extracellular environment, necessitating cycles of engagement and disengagement of integrin bonds to the extracellular matrix.<sup>33</sup> Thus, the presence of  $\alpha v\beta 3$  integrin clusters in FAs of cells adhering to the  $\alpha 5\beta 1$  integrin selective ligand could be explained, considering that  $\alpha v\beta 3$  integrin clusters are physically necessary to stabilize FAs and to link to actin fibers, even when these integrins are not bound to the ligand on the surface (Fig. 3). It should be also noted that on the nanopatterned substrates cells cannot assemble extracellular matrix because of the presence of the polyethylene glycol layer between the nanoparticles, which prevents any protein binding and adsorption. Thus, the fibrillar structures formed in cells adhering to the  $\alpha 5\beta 1$  ligand should not be considered as functional fibrillar adhesion arising from the translocation of  $\alpha 5\beta 1$  integrins upon assembly of extracellular matrix fibers.<sup>2,5</sup>

Here, we demonstrated that the clustering behavior and selective binding of  $\alpha 5\beta 1$  and  $\alpha v\beta 3$  integrins regulate cell adhesion and FA assembly. We achieved spatial control of integrin clustering type by using a tool for surface nanopatterning of integrin ligands, which enables precise control of receptor localization. However, the mechanism underlying the spatio-temporal regulation of bound and non-bound integrins in FAs still remains unclear. The current understanding of FA molecular composition is limited, though recent studies using high-resolution microscopy have begun to elucidate the dynamics of FAs at the nanoscale, and its impact on signaling. Combining our nanopatterning tools with high-resolution microscopy approaches will enable us to elucidate the specific dynamics of  $\alpha 5\beta 1$  and  $\alpha v\beta 3$  integrins localized in a FA, by means of controlled ligand/receptor spatial organization. Thus, it would be possible to determine not only the spatial organization of single bound and non-bound integrins, but also how different integrin types signal each other, in response to chemical and physical properties of the extracellular matrix. Future studies should also clarify the effects of integrin mobility and spatial organization in clusters on cell signaling responses.

## Materials and methods

### Preparation and functionalization of nanopatterned surfaces

Nanopatterned substrates were prepared by block copolymer micelle nanolithography, as previously described.<sup>34,35</sup> Briefly, glass coverslips were either dip-

coated or spin-coated with a monolayer of polystyrene-block-poly[2-vinylpyridine(HAuCl<sub>4</sub>)] (Sigma Aldrich 520918 H<sub>2</sub>AuCl<sub>4</sub>) diblock copolymer micelles in *o*-xylene. To obtain the interparticle distances of 30, 60 and 90 nm, polystyrene (288)-block-poly (2-vinylpyridine) (119), polystyrene (1056)-block-poly (2-vinylpyridine) (671) and polystyrene (1824)-block-poly (2-vinylpyridine)(523) (Polymer Source Inc. P4554-S2VP) were used. Following plasma treatment, the gold ions on the surfaces were reduced to gold and the polymer micelles were removed, resulting in quasi-hexagonal patterns of gold nanoparticles. To prevent cell adhesion and protein deposition between these nanoparticles, substrates were passivated with polyethylene glycol (PEG) (2000)-triethoxysilane.<sup>36</sup> The nanoparticles were then functionalized with the integrin selective peptidomimetic ligands, which bind either  $\alpha 5\beta 1$  or  $\alpha v\beta 3$  integrins, at a concentration of 25  $\mu$ M in MilliQ water for 4 hr at room temperature.<sup>16</sup> The unbound ligands were removed by gentle shaking, and the samples were thoroughly rinsed with MilliQ water overnight. The surfaces were further washed with sterile PBS, prior to cell experiments. To characterize the patterned surfaces, the samples were imaged with scanning electron microscopy (LEO 1530 Gemini, Carl Zeiss). The interparticle distances and the order of the hexagonal patterns were determined by analyzing the micrographs with a custom-made Image J plug-in, written by Dr. Philippe Girard (University of Heidelberg).

### Cell cultures

Human osteosarcoma U2OS cells (ATCC, HTB-96) were cultured in DMEM supplemented with 10% FBS, 1% L-glutamine and 1% penicillin streptomycin (all from Gibco Laboratories, 10938-025, 10500-064, 25030-024, 15140-122) at 37°C and 5% CO<sub>2</sub>. Prior to the experiments, cells were serum starved overnight. During the experiments, cells were gently detached with Accutase (Gibco, A11105-01) and seeded at a density of 600 cells/mm<sup>2</sup> in DMEM supplemented with 1% FBS. For transfection, cells were seeded at a density of  $1 \times 10^5$  cells/well in a 6-well plate, until they reached 80% confluency. Cells were transfected using Lipofectamin 2000 (Invitrogen 11668027) and 2  $\mu$ g  $\alpha v$ -mApple plasmid (Addgene 54866) in Opti-MEM (Gibco 31985-062) for 32 hr. Cells were then detached with Trypsin (Gibco, 25300-054) and plated on the nanopatterned surfaces.

### Cell adhesion and spreading analysis

U2OS cells were seeded on the substrates, and allowed to adhere for 10 min. Time-lapse



microscopy was then carried out at 37°C and 5% CO<sub>2</sub>. Phase contrast images of 5 random fields from each sample were acquired every 10 min over a period of 8 hr, using a DeltaVision RT system (Applied Precision, Inc.) on an Olympus IX inverted microscope equipped with a 20x/0.50 Ph1 UPlanFl. Cell imaging was carried out with a cooled CCD camera (Photometrics); images were acquired with the Resolve 3D program. ImageJ software, version 1.48v (Rasband, W.S., ImageJ, U. S. National Institutes of Health, Bethesda, Maryland, USA, <http://rsb.info.nih.gov/ij/>, 1997-2009) was used to: (i) measure cell area; (ii) generate kymographs (using the Multiple Kymograph Plug-in from J. Rietdorf, FMI Basel, and A. Seitz, EMBL Heidelberg); and (iii) adjust image brightness and contrast levels for presentation. Data (cell n = 15 for the 30 nm particle spacing; n = 22 for the 60 nm spacing; and n = 15 for the 90 nm spacing) were plotted in OriginLab 9.1; standard deviations and standard errors of the mean were calculated with the same software.

### **Immunocytochemical staining and fluorescence microscopy**

For immunocytochemical staining, cells were plated for 4 hr on the nanopatterned surfaces. Cells were then washed with warm PBS, and fixed in 3.7% paraformaldehyde in PBS for 20 min. Post-fixation, cells were permeabilized with 0.1% TritonX-100 in PBS for 5 min, blocked with 1% bovine serum albumin (BSA) in PBS, and incubated for 1 hr with the following antibodies: mouse anti-human  $\alpha v \beta 3$  integrin (Millipore, MAB1976), rat anti-human  $\alpha 5$ -integrin (MABII, kindly provided by K. Yamada), mouse anti-human vinculin (Sigma, V9131), and rabbit anti-human zyxin (Synaptic Systems, 307011). Actin stress fibers were labeled with phalloidin-TRITC (Sigma, P1951). To visualize labeled membrane proteins, fixed cells were treated with secondary antibodies for 45 min (Invitrogen A-21238, A-11006, A-11001, A-11078). After washing with PBS, coverslips were mounted in Elvanol (Mowiol 4-88, Karl Roth & Co GmbH, 0713.1). Immunofluorescent images were obtained with the Delta Vision Spectris System, as described above. Cells were examined with a 60x/1.4 UPlanApo oil immersion objective (Olympus).

Focal adhesion size was measured by using ImageJ 1.48v; the results of the measurements were displayed in a box plot plotted with OriginLab 9.1. The statistical significance of variation in focal adhesion size for the different groups was determined by applying the Mann-Whitney U test in GraphPad Prism, version 6.0.

### **Integrin blocking experiments**

For integrin blocking experiments, cells were resuspended in DMEM containing 1% FBS and 1% BSA. Afterwards, 100  $\mu$ l of the cell suspension ( $1 \times 10^6$  cells/ml) was incubated with 10  $\mu$ l of thiol-free ligands (25  $\mu$ M) for 30 min at 4°C. The cells were then plated on substrates functionalized with  $\alpha 5 \beta 1$ - or  $\alpha v \beta 3$  integrin selective ligands, and fixed after 4 hr. Prior to fixation, samples were rinsed twice with PBS to remove unattached cells. Fixed cells were stained, as described above in the previous paragraph on immunocytochemical staining.

### **Abbreviations**

ECM	Extracellular matrix
FAs	focal adhesions
PEG	polyethylene glycol

### **Disclosure of potential conflicts of interest**

No potential conflicts of interest were disclosed.

### **Acknowledgments**

We thank Mrs. Barbara Morgenstern for her invaluable editorial help with the manuscript, and Dr. Janet Askari (University of Manchester, UK) for helpful discussions. J.P.S. is the Weston Visiting Professor at the Weizmann Institute of Science, and is a member of the Heidelberg Cluster of Excellence CellNetworks. B.G is the Erwin Neter Professor of Cell and Tumor Biology. A. C.A. and J.P.S. are members of the collaborative research cluster SFB1129 from the German Research Foundation.

### **Funding**

Financial support was provided by the European Research Council under the European Union's Seventh Framework Program (FP/2007-2013)/ERC Grant Agreement no. 294852, and the BMBF/MPG network MaxSynBio.

### **References**

- [1] Geiger B, Spatz JP, Bershadsky AD. Environmental sensing through focal adhesions. *Nat Rev Mol Cell Biol* 2009; 10:21-33; PMID:19197329; <http://dx.doi.org/10.1038/nrm2593>
- [2] Zamir E, Katz M, Posen Y, Erez N, Yamada KM, Katz B-Z, Lin S, Lin DC, Bershadsky AD, Kam Z, et al. Dynamics and segregation of cell-matrix adhesions in cultured fibroblasts. *Nat Cell Biol* 2000; 2:191-6; PMID:10783236; <http://dx.doi.org/10.1038/35008607>
- [3] Danen EHJ, Sonneveld P, Brakebusch C, Fässler R, Sonnenberg A. The fibronectin-binding integrins alpha5-beta1 and alphavbeta3 differentially modulate RhoA-GTP loading, organization of cell matrix adhesions, and

- fibronectin fibrillogenesis. *J Cell Biol* 2002; 159:1071-86; PMID:12486108; <http://dx.doi.org/10.1083/jcb.2002.05014>
- [4] Roca-Cusachs P, Gauthier N, del Rio A, Sheetz MP. Clustering of  $\alpha 5 \beta 1$  integrins determines adhesion strength whereas  $\alpha v \beta 3$  and talin enable mechanotransduction. *Proc Natl Acad Sci USA* 2009; 106:16245-50; PMID:19805288; <http://dx.doi.org/10.1073/pnas.090.2818106>
- [5] Pankov R, Cukierman E, Katz B-Z, Matsumoto K, Lin DC, Lin S, Hahn C, Yamada KM. Integrin dynamics and matrix assembly: tensin-dependent translocation of  $\alpha 5 \beta 1$  integrins promotes early fibronectin fibrillogenesis. *J Cell Biol* 2000; 148:1075-90; PMID:10704455; <http://dx.doi.org/10.1083/jcb.148.5.1075>
- [6] Geiger B, Yamada KM. Molecular architecture and function of matrix adhesions. *Cold Spring Harb Perspect Biol* 2011; 3:1-21; PMID:21441590; <http://dx.doi.org/10.1101/cshperspect.a005033>
- [7] Rossier O, Oceau V, Sibarita J-B, Leduc C, Tessier B, Nair D, Gatterdam V, Destaing O, Albigès-Rizo C, Tampé R, et al. Integrins  $\beta 1$  and  $\beta 3$  exhibit distinct dynamic nanoscale organizations inside focal adhesions. *Nat Cell Biol* 2012; 14:1057-67; PMID:23023225; <http://dx.doi.org/10.1038/ncb2588>
- [8] Friedland JC, Lee MH, Boettinger D. Mechanically activated integrin switch controls  $\alpha 5 \beta 1$  function. *Science* 2009; 323:642-4; PMID:19179533; <http://dx.doi.org/10.1126/science.1168441>
- [9] Schiller HB, Hermann M-R, Polleux J, Vignaud T, Zanivan S, Friedel CC, Sun Z, Raducanu A, Gottschalk K-E, Théry M, et al.  $\beta 1$ - and  $\alpha v$ -class integrins cooperate to regulate myosin II during rigidity sensing of fibronectin-based microenvironments. *Nat Cell Biol* 2013; 15:625-36; PMID:23708002; <http://dx.doi.org/10.1038/ncb2747>
- [10] Morgan MR, Byron A, Humphries MJ, Bass MD. Giving off mixed signals—distinct functions of  $\alpha 5 \beta 1$  and  $\alpha v \beta 3$  integrins in regulating cell behaviour. *IUBMB Life* 2009; 61:731-8; PMID:19514020; <http://dx.doi.org/10.1002/iub.200>
- [11] Wolfenson H, Bershadsky A, Henis YI, Geiger B. Actomyosin-generated tension controls the molecular kinetics of focal adhesions. *J Cell Sci* 2011; 124:1425-32; PMID:21486952; <http://dx.doi.org/10.1242/jcs.077388>
- [12] Lin GL, Cohen DM, Desai RA, Breckenridge MT, Gao L, Humphries MJ, Chen CS. Activation of  $\beta 1$  but not  $\beta 3$  integrin increases cell traction forces. *FEBS Lett* 2013; 587:763-9; PMID:23395612; <http://dx.doi.org/10.1016/j.febslet.2013.01.068>
- [13] Rahmouni S, Lindner A, Rechenmacher F, Neubauer S, Sobahi TRA, Kessler H, Cavalcanti-Adam EA, Spatz JP. Hydrogel micropillars with integrin selective peptidomimetic functionalized nanopatterned tops: a new tool for the measurement of cell traction forces transmitted through  $\alpha v \beta 3$ - or  $\alpha 5 \beta 1$ -integrins. *Adv Mater* 2013; 25:5869-74; PMID:23913640; <http://dx.doi.org/10.1002/adma.201301338>
- [14] Balcioglu HE, van Hoorn H, Donato DM, Danen EHJ, Erik. Integrin expression profile modulates orientation and dynamics of force transmission at cell matrix adhesions. *J Cell Sci* 2015; 128:1316-26; PMID:25663698; <http://dx.doi.org/10.1242/jcs.156950>
- [15] Mould AP, Craig SE, Byron SK, Humphries MJ, Jowitt TA. Disruption of integrin–fibronectin complexes by allosteric but not ligand-mimetic inhibitors. *Biochem J* 2014; 464:301-13; PMID:25333419; <http://dx.doi.org/10.1042/BJ20141047>
- [16] Rechenmacher F, Neubauer S, Polleux J, Mas-Moruno C, De Simone M, Cavalcanti-Adam EA, Spatz JP, Fässler R, Kessler H. Functionalizing  $\alpha v \beta 3$ - or  $\alpha 5 \beta 1$ -selective integrin antagonists for surface coating: A method to discriminate integrin subtypes in vitro. *Angew Chem Int Ed* 2012; 52:1572-5; PMID:23345131; <http://dx.doi.org/10.1002/anie.201206370>
- [17] Guasch J, Conings B, Neubauer S, Rechenmacher F, Ende K, Rolli CG, Kappel C, Schaufler V, Micoulet A, Kessler H, et al. Segregation versus colocalization: orthogonally functionalized binary micropatterned substrates regulate the molecular distribution in focal adhesions. *Adv Mater* 2015; 27:3737-47; PMID:25981929; <http://dx.doi.org/10.1002/adma.201500900>
- [18] Fraioli R, Rechenmacher F, Neubauer S, Manero JM, Gil J, Kessler H, Mas-Moruno C. Mimicking bone extracellular matrix: integrin-binding peptidomimetics enhance osteoblast-like cells adhesion, proliferation, and differentiation on titanium. *Colloids Surf B* 2015; 128:191-200; PMID:25637448; <http://dx.doi.org/10.1016/j.colsurfb.2014.12.057>
- [19] Cluzel C, Saltel F, Lussi J, Paulhe F, Imhof BA, Wehrle-Haller B. The mechanisms and dynamics of ( $\alpha$ )v ( $\beta$ )3 integrin clustering in living cells. *J Cell Biol* 2005; 171:383-92; PMID:16247034; <http://dx.doi.org/10.1083/jcb.200503017>
- [20] Askari JA, Tynan CJ, Webb SED, Martin-Fernandez ML, Ballestrem C, Humphries MJ. Focal adhesions are sites of integrin extension. *J Cell Biol* 2010; 188:891-903; PMID:20231384; <http://dx.doi.org/10.1083/jcb.2009.07174>
- [21] Arnold M, Cavalcanti-Adam EA, Glass R, Blümmel J, Eck W, Kantelechner M, Kessler H, Spatz JP. Activation of integrin function by nanopatterned adhesive interfaces. *ChemPhysChem* 2004; 5:383-8; PMID:15067875; <http://dx.doi.org/10.1002/cphc.200301014>
- [22] Cavalcanti-Adam EA, Volberg T, Micoulet A, Kessler H, Geiger B, Spatz JP. Cell spreading and focal adhesion dynamics are regulated by spacing of integrin ligands. *Biophys J* 2007; 92:2964-74; PMID:17277192; <http://dx.doi.org/10.1529/biophysj.106.089730>
- [23] Liu Y, Medda R, Liu Z, Galior K, Yehl K, Spatz JP, Cavalcanti-Adam EA, Salaita K. Nanoparticle tension probes patterned at the nanoscale: Impact of integrin clustering on force transmission. *Nano Lett* 2014; 14:5539-46; PMID:25238229; <http://dx.doi.org/10.1021/nl501912g>
- [24] Zaidel-Bar R, Milo R, Kam Z, Geiger B. A paxillin tyrosine phosphorylation switch regulates the assembly and form of cell-matrix adhesions. *J Cell Sci* 2006; 120:137-48; PMID:17164291; <http://dx.doi.org/10.1242/jcs.03314>
- [25] LaFlamme SE, Akiyama SK, Yamada KM. Regulation of fibronectin receptor distribution. *J Cell Biol* 1992; 117:437-47; PMID:1373145; <http://dx.doi.org/10.1083/jcb.117.2.437>

- [26] Neubauer S, Rechenmacher F, Beer AJ, Curnis F, Pohle K, D'Alessandria C, Wester H-J, Reuning U, Corti A, Schwaiger M, et al. Selective imaging of the angiogenic relevant integrins  $\alpha 5\beta 1$  and  $\alpha v\beta 3$ . *Angew Chem Int Ed* 2013; 52:11656-9; PMID:24115324; <http://dx.doi.org/10.1002/anie.201306376>
- [27] de Beer AGF, Cavalcanti-Adam EA, Majer G, Lopez-García M, Kessler H, Spatz JP. Force-induced destabilization of focal adhesions at defined integrin spacings on nanostructured surfaces. *Phys Rev E* 2010; 81:051914-7; PMID:20866268; <http://dx.doi.org/10.1103/PhysRevE.81.051914>
- [28] Rechenmacher F, Neubauer S, Mas-Moruno C, Dorfner PM, Polleux J, Guasch J, Conings B, Boyen H-G, Bochen A, Sobahi TR, et al. A molecular toolkit for the functionalization of titanium-based biomaterials that selectively control integrin-mediated cell adhesion. *Chem Eur J* 2013; 19:9218-23; PMID:23744802; <http://dx.doi.org/10.1002/chem.201301478>
- [29] Charo IF, Nannizzi L, Smith JW, Cheresch DA. The vitronectin receptor  $\alpha v\beta 3$  binds fibronectin and acts in concert with  $\alpha 5\beta 1$  in promoting cellular attachment and spreading on fibronectin. *J Cell Biol* 1990; 111:2795-800; PMID:1703545; <http://dx.doi.org/10.1083/jcb.111.6.2795>
- [30] Dobereiner HG, Dubin-Thaler BJ, Giannone G, Sheetz MP. Force sensing and generation in cell phases: analyses of complex functions. *J Appl Physiol* 2005; 98:1542-6; PMID:15772064; <http://dx.doi.org/10.1152/jappphysiol.01181.2004>
- [31] Davey G, Buzzai M, Assoian RK. Reduced expression of  $\alpha 5\beta 1$  integrin prevents spreading-dependent cell proliferation. *J Cell Sci* 1999; 112:4663-72; PMID:10574714
- [32] Kanchanawong P, Shtengel G, Pasapera AM, Ramko EB, Davidson MW, Hess HF, Waterman CM. Nanoscale architecture of integrin-based cell adhesions. *Nature* 2010; 468:580-4; PMID:21107430; <http://dx.doi.org/10.1038/nature09621>
- [33] Case LB, Waterman CM. Adhesive F-actin waves: A novel integrin-mediated adhesion complex coupled to ventral actin polymerization. *PLoS One* 2011; 6:e26631-13; PMID:22069459; <http://dx.doi.org/10.1371/journal.pone.0026631>
- [34] Spatz JP, Mössmer S, Hartmann C, Möller M, Herzog T, Krieger M, Boyen H-G, Ziemann P, Kabius B. Ordered deposition of inorganic clusters from micellar block copolymer films. *Langmuir* 2000; 16:407-15; <http://dx.doi.org/10.1021/la990070n>
- [35] Glass R, Möller M, Spatz JP. Block copolymer micelle nanolithography. *Nanotechnology* 2003; 14:1153-60; <http://dx.doi.org/10.1088/0957-4484/14/10/314>
- [36] Blümmel J, Perschmann N, Aydin D, Drinjakovic J, Surrey T, López-García M, Kessler H, Spatz JP. Protein repellent properties of covalently attached PEG coatings on nanostructured SiO<sub>2</sub>-based interfaces. *Biomaterials* 2007; 28:4739-47; PMID:17697710; <http://dx.doi.org/10.1016/j.biomaterials.2007.07.038>